◆ Human Brain Mapping 38:2260–2275 (2017) ◆

Quantifying the Variability of Scene-Selective Regions: Interindividual, Interhemispheric, and Sex Differences

Zonglei Zhen,[1] Xiang-Zhen Kong,[1] Lijie Huang,[1] Zetian Yang,[1] Xu Wang,[1] Xin Hao,[1] Taicheng Huang,[1] Yiying Song,[1] and Jia Liu [2]*

[1]*State Key Laboratory of Cognitive Neuroscience and Learning & IDG/McGovern Institute for Brain Research, Beijing Normal University, Beijing, 100875, China*
[2]*School of Psychology, Beijing Normal University, Beijing, 100875, China*

Abstract: Scene-selective regions (SSRs), including the parahippocampal place area (PPA), retrosplenial cortex (RSC), and transverse occipital sulcus (TOS), are among the most widely characterized functional regions in the human brain. However, previous studies have mostly focused on the commonality within each SSR, providing little information on different aspects of their variability. In a large group of healthy adults ($N = 202$), we used functional magnetic resonance imaging to investigate different aspects of topographical and functional variability within SSRs, including interindividual, interhemispheric, and sex differences. First, the PPA, RSC, and TOS were delineated manually for each individual. We then demonstrated that SSRs showed substantial interindividual variability in both spatial topography and functional selectivity. We further identified consistent interhemispheric differences in the spatial topography of all three SSRs, but distinct interhemispheric differences in scene selectivity. Moreover, we found that all three SSRs showed stronger scene selectivity in men than in women. In summary, our work thoroughly characterized the interindividual, interhemispheric, and sex variability of the SSRs and invites future work on the origin and functional significance of these variabilities. Additionally, we constructed the first probabilistic atlases for the SSRs, which provide the detailed anatomical reference for further investigations of the scene network. *Hum Brain Mapp 38:2260–2275, 2017*.

Key words: scene-selective regions (SSRs); interindividual variability; individual differences; interhemispheric differences; sex differences

Additional Supporting Information may be found in the online version of this article.

Contract grant sponsor: National Natural Science Foundation of China; Contract grant number: 31230031; Contract grant sponsor: National Basic Research Program of China; Contract grant number: 2014CB846101; Contract grant sponsor: National High-tech R&D Program of China; Contract grant number: 2015AA020514; Contract grant sponsor: National Natural Science Foundation of China; Contract grant numbers: 31221003, 31471067, and 31470055; Contract grant sponsor: National Social Science Foundation of China; Contract grant numbers: 13&ZD073, 14ZDB160; Contract grant sponsor: Changjiang Scholars Programme of China.

Zonglei Zhen and Xiang-Zhen Kong contributed equally to this work.

Conflict of Interest: None declared.

*Correspondence to: Jia Liu, School of Psychology, Beijing Normal University, Beijing 100875, China. E-mail: liujia@bnu.edu.cn

Received for publication 2 April 2016; Revised 3 January 2017; Accepted 4 January 2017.

DOI: 10.1002/hbm.23519

Published online 24 January 2017 in Wiley Online Library (wileyonlinelibrary.com).

INTRODUCTION

Scene recognition is a highly developed skill in humans which is critical to navigating our world. We can recognize a scene with a single glance, and seamlessly integrate that information for use in spatial navigation. Using functional magnetic resonance imaging (fMRI), three cortical regions of the human brain have been repeatedly identified as specialized scene-processing areas. These are the parahippocampal cortex (PHC, or parahippocampal place area [PPA]) [Aguirre et al., 1996; Epstein and Kanwisher, 1998], the retrosplenial complex (RSC) [Bar and Aminoff, 2003; Maguire, 2001], and the transverse occipital sulcus (TOS, or occipital place area [OPA]) [Dilks et al., 2013; Grill-Spector, 2003]. These regions respond more strongly to scenes (e.g., landscapes, cityscapes, rooms) than to non-scenes, and have therefore been called scene-selective regions (SSRs). Over the past two decades, great efforts have been made in characterizing the precise function of these SSRs, with current hypotheses suggesting that these regions play distinct but complementary roles in spatial navigation. For example, the PPA may encode the spatial layout of the scenes [Epstein, 2008; Epstein et al., 1999, 2007; Henderson et al., 2008; Kravitz et al., 2011; Park et al., 2011], while the RSC may support memory retrieval for the location of a scene situated within the broader spatial environment [Epstein, 2008; Epstein et al., 2007; Suzuki et al., 1998; Wolbers and Buchel, 2005], and the TOS may be involved in initial stages of scene processing [Aminoff and Tarr, 2015; Bettencourt and Xu, 2013; Dilks et al., 2013; MacEvoy and Epstein, 2007]. Despite the advances in understanding the specific function of each SSR, most previous studies focus on spatial and functional commonalities within each SSR, devoting very little effort to characterizing the variability of SSRs across individuals, sex, or even hemispheres. Here, with a large cohort of healthy adults, we used fMRI to investigate the different aspects of variability of the SSRs.

One notable aspect of variability is interindividual difference in spatial topography and functional selectivity of the SSRs. Cytoarchitectonic mapping has revealed a considerable degree of intersubject variability in the location and extent of anatomically defined regions throughout the cortex [Amunts et al., 1999; Caspers et al., 2013; Scheperjans et al., 2008; Zilles and Amunts, 2013]. Cortical surface reconstructions from structural MRI have also revealed significant interindividual variability in cortical shape and folding [Fischl et al., 2008; Hill et al., 2010; Van Essen and Dierker, 2007]. More importantly, interindividual variability has provided information vital for our understanding of the neural basis of complex behaviors, including spatial navigation. For example, interindividual variability of hippocampal volume in taxi drivers has been correlated with their amount of time spent as a taxi driver [Maguire et al., 2000, 2006], and the differences in hippocampal volume predict individual differences in drivers' ability to learn the cognitive maps [Schinazi et al., 2013]. Although a large amount of work is being devoted to assessing interindividual variability in anatomically defined navigation-related regions such as the hippocampus, the interindividual variability of functionally defined navigation-related regions such as the SSRs is rarely quantified. Indeed, to the best of our knowledge, only one study has characterized interindividual variability within the SSRs [Frost and Goebel, 2012]. The study reveals significant spatial variability in the PPA; however, it does not characterize its functional variability or SSRs other than the PPA. Additionally, the study utilizes a very small sample size (i.e., 10 subjects). Therefore, as yet there is no comprehensive description of interindividual variability for the three widely studied SSRs.

In addition to the variability across individuals, previous studies reveal that, even in a single subject, the brain shows appreciable variability between two hemispheres [Gotts et al., 2013; Herve et al., 2013; Toga and Thompson, 2003]. The interhemispheric differentiation is frequently indicative of functional specialization of the brain, particularly in the cortex [Chance, 2014; Hellige, 1990; Hugdahl, 2011]. It has been shown that in scene perception, the left hemisphere preferentially processes categorical spatial relationships, while the right preferentially processes coordinate spatial relationships [Jager and Postma, 2003; Van der Ham et al., 2011]. Notably, interhemispheric differences have been identified in anatomically defined navigation-related regions. For example, the right hippocampus is solely activated when taxi drivers recall the complex routes [Maguire et al., 1997]. However, whether there exist interhemispheric differences in the functionally-defined navigation-related regions (i.e., SSRs) is still unknown.

Finally, sex differences in spatial navigation have been frequently reported in previous studies [Astur et al., 1998; Linn and Petersen, 1985; Lovden et al., 2007; Moffat et al., 1998; Rahman et al., 2005]. Studies comparing group differences between the sexes have identified greater advantage for men in processing specific spatial navigation tasks such as wayfinding via map [Cherney et al., 2008; Malinowski and Gillespie, 2001] or accurately sensing direction[Chai and Jacobs, 2009]. Neuroimaging studies have revealed abundant sex differences in both brain structure and function related to navigation, including structural differences in hippocampal size [Persson et al., 2014], and functional differences in regional activation during a maze task [Gron et al., 2000; Nowak et al., 2011; Sneider et al., 2011], suggesting that men and women recruit different brain regions for spatial navigation. However, it remains unclear whether SSRs as a critical early-stage component of spatial navigation show sex differences.

Given the variability described above for navigation-related brain regions, we hypothesize that each SSR should have similar variability in the interindividual, interhemispheric, and sex domains. This study aimed to use fMRI to characterize such variabilities in all three well-studied SSRs, and in a large sample of healthy subjects ($N = 202$). Subjects underwent scans while viewing navigationally relevant scenes. To characterize the variability of SSRs, a series of

analysis was conducted. First, all three SSRs were delineated manually for each individual in each hemisphere. Second, the interindividual variability of SSRs was quantified in its spatial topography and functional selectivity. Finally, the interhemispheric and sex differences in the spatial topography and functional selectivity were examined for the SSRs.

MATERIALS AND METHODS

Data Description

Subjects

Two hundred and two college students (124 females; mean age = 20.3 years, standard deviation [SD] = 0.88 years) from Beijing Normal University, China, participated in this study as a part of our ongoing project to explore the association between brain, cognitive functions, and genetics. Among them, 173 described themselves as right-handed, and 29 described themselves as left-handed. All subjects had normal or corrected-to-normal vision. The study was approved by the Institutional Review Board of Beijing Normal University. Written informed consent was obtained from all subjects before they took part in the experiment.

Localizer paradigm

A dynamic scene localizer task was used to define the SSRs [Fox et al., 2009]. Specifically, the dynamic localizer consisted of three blocked-design functional runs, each of which lasted 198 s. Each run contained two block sets, intermixed with three 18-s rest blocks at the beginning, middle, and end of the run. Each block set consisted of one block for each of four stimulus categories (i.e., faces, scenes, objects, and scrambled objects), with each stimulus category presented in an 18-s block. Each block consisted of six 3-s movie clips, which were randomly drawn from a pool of 60 clips [for more details on the stimuli, see Pitcher et al., 2011]. The order of stimulus category blocks in each run was palindromic and randomized across runs. During scanning, subjects were instructed to passively view movie clips. For this study, we defined the SSRs by the contrast between scenes and objects. The characterization for the variability of face-selective regions (FSRs) using the same dataset was reported separately [Zhen et al., 2015].

Image Acquisition

All MR imaging was done at the BNU Imaging Center for Brain Research, Beijing, China, on a Siemens 3T whole-body scanner (MAGENTOM Trio, a Tim system) with a 12-channel phased-array head coil. Functional blood-oxygen-level-dependent (BOLD) images were acquired with a T2*-weighted gradient-echo, echo-planar-imaging (GRE-EPI) sequence (TR = 2 s, echo time = 30 ms, flip angle = 90°, in-plane resolution = 3.1 × 3.1 mm). Whole-brain coverage for the functional data was obtained using 30 contiguous interleaved 4.8 mm axial slices. Structural T1-weighted images were acquired with a 3D magnetization-prepared rapid acquisition gradient echo (MP-RAGE) sequence (TR/TE/TI = 2,530/3.39/1,100 ms, flip angle = 7°) for spatial normalization. Earplugs were used to attenuate scanner noise, and head motion was restrained with a foam pillow and extendable padded head clamps.

Quality Control

Two predefined criteria were used to assess the quality of functional MR images. First, subjects' images with excessive motion (>2 mm in translation or >2° in rotation) were tagged, and if more than 20 volumes across all runs were tagged, the subject was excluded from the further analysis. Second, structure-function misalignment error was reduced by excluding subjects with a large error of registration. Registration quality was checked visually by overlaying the normalized functional volume on the MNI152 template. After assessment, no subjects required exclusion (i.e., no large motion or misalignment errors).

Image Processing

Activation analysis

Functional images were analyzed with FEAT (FMRI Expert Analysis Tool) Version 5.98, part of FSL (FMRIB's Software Library, www.fmrib.ox.ac.uk/fsl). First-level analysis was conducted separately on each run and each session (i.e., subject). Preprocessing included motion correction, brain extraction, spatial smoothing with a Gaussian kernel (FWHM = 6 mm), grand-mean intensity normalization, and high-pass temporal filtering (120 s cutoff). Statistical analyses on time series were performed using FILM (FMRIB's Improved Linear Model) with a local autocorrelation correction. A boxcar kernel was convolved with a gamma hemodynamic response function, and its temporal derivative was used to model BOLD signal changes. Six parameters from motion-correction were also included in the model as regressors of no interest, to account for the effect of head movements. A second-level fixed-effect analysis was done to combine all runs within each session. Specifically, the parameter (i.e., beta) image from the first-level analysis was firstly aligned to the individual's structural images through FLIRT (FMRIB's linear image registration tool) with 6 degrees of freedom, and then warped to the MNI152 template through FNIRT (FMRIB's nonlinear image registration tool) running with default parameters. The spatially normalized parameter images (resampled to 2-mm isotropic voxels) were then summarized across runs in each session using a fixed-effect model. The statistic images from the second-level analysis were then used to delineate the subject-specific SSRs for each subject.

Subject-specific SSR delineation

We focused on the SSRs located in the occipitotemporal cortex, including the PPA, TOS, and RSC. The subject-specific

SSRs were delineated manually in the parcel unit based on the individual activation map from the contrast of scenes versus objects. The subject-specific activation image was first thresholded ($Z > 2.3$, uncorrected) and partitioned into many small parcels with the watershed algorithm. The watershed algorithm partitions an image by analogous process of a landscape being flooded by water in which water seeps in from every local minimum and the landscape is finally divided into multiple regions separated by the watersheds [Meyer, 1994]. Here, the activation map was treated as the landscape, and the watershed lines were the borders among different local homogenous regions (parcels). As a result, a set of parcels were generated from the partition. Then, the raters hand-picked the parcels on the individual activation map to construct the SSRs following a standard procedure. First, the gyri and sulcus from MNI152 template were used as the anatomical landmarks to locate the SSRs coarsely [Nasr et al., 2011]. Specifically, the PPA was located near the lateral lip of the collateral sulcus and adjacent medial fusiform gyrus; the TOS was centered on the lateral occipital gyrus, anterior and ventral to the transverse occipital sulcus; and the RSC was located in the fundus of the parieto-occipital sulcus. Second, we used the SSR group labels (i.e., the functional landmark, see Supporting Information Fig. S1) as a spatial extent reference. The major part of each candidate parcel overlapped with or neighbored to the corresponding functional label. Finally, from the parcels that showed good correspondence to both anatomical and functional landmarks, we identified the one with the strongest scene-selective activation as the center of a SSR, and iteratively merged the parcels which connected with the selected parcels into the regions until no candidate parcels met the criteria. A specialized tool, called FreeROI (http://freeroi.brainactivityatlas.org), was developed in Python to aid the raters in delineating regions of interest (ROI).

To speed up the delineation and avoid biases from individual raters, seven raters (i.e., the first seven authors) took part in delineating the SSRs in four phases. First, the brains were randomly divided into seven approximately equal subsets, each of which was assigned to one rater for delineating the SSRs. Second, each subset was assigned to another rater for re-delineating the SSRs. Third, the delineated SSRs from the first two phases were double-checked and refined by the two raters who had delineated it. Finally, SSRs that could not be resolved by the two raters were evaluated by all seven raters and finalized together.

Reliability of intra- and inter-rater delineation

In order to evaluate the reliability of the delineation procedure, both the inter- and intra-rater reliability for each SSR were assessed with Dice's coefficient, the ratio of twice the number of overlapping voxels from two different delineations divided by the sum of the total number of voxels in the two delineations. Inter-rater reliability was based on the two delineations, that were produced by the two different raters in the first two phases described above. Intra-rater reliability was assessed by having each rater re-delineate the SSRs for the same subset that rater assessed in the first phase, several weeks after the first delineation. These were then compared to compute intra-rater reliability. Finally, a paired *t*-test was used to test whether there were significant differences between the inter-rater and intra-rater reliability of the delineations.

Interindividual Variability in SSRs

Spatial topography

To characterize the spatial variability of SSRs, a probabilistic atlas (or map) was first created for each SSR, by calculating the frequency of a respective SSR being present at a given position across all subjects. The map coded the occurrence probability of each voxel being located in the SSR, and thus provided a voxel-wise description for inter-individual variability in the location and extent of that SSR. In addition, a maximum-probability map (MPM) was constructed to integrate the multiple probabilistic SSR maps into one map, and to characterize the spatial relations among SSRs. Specifically, for each voxel, we compared its values from each probabilistic map, and assigned that voxel to the SSR which showed the highest probability at the voxel. If one voxel showed equal probabilities for multiple SSRs, it would be assigned to the SSR, which owned the highest average probability in the 26 immediate neighbors of the voxel. The voxels with a maximal probability below 10% were set to 0, indicating that they most likely did not belong to any SSR. As a result, the MPM defined the most likely SSR to which each voxel belonged.

Interindividual variability of spatial topography of the SSRs was further characterized according to the MNI stereotaxic coordinates of peak activation. Specifically, for each SSR, the coordinates of peak activation were identified in each subject, and the mean coordinates of all peaks were calculated as the center of the peak locations. The standard deviation (SD) of the coordinates on each axis was calculated for each SSR to measure the interindividual dispersion of the locations of peak activation. The sum of the three SDs for each SSR was further calculated as a measure of the overall variability of peak locations in MNI stereotaxic space.

Scene selectivity

Functional variability of SSRs was evaluated in terms of scene selectivity. Scene selectivity for a voxel was defined as percent signal change (PSC) between scenes versus objects:

$$\mathrm{PSC} = \frac{\beta_s - \beta_o}{\beta_{mean}} * 100$$

where β_s, β_o, and β_{mean} refer to the beta values for the scenes, the objects, and the mean intensity of the baseline

(the intercept), respectively, which were in turn calculated from the fixed-effects GLM. To avoid influence by the region size, we focused on the peak voxel, which showed the strongest scene selectivity within a subject-specific SSR. The coefficient of variation (CV = SD/mean) was used to quantify the interindividual variability of scene selectivity in each SSR.

Interhemispheric Differences in SSRs

Spatial topography

As the spatial extents of SSRs are largely affected by the threshold used to define them, the interhemispheric differences of SSRs were characterized based on the locations of peak activation. Specifically, for each SSR, the coordinates of the peak activation were identified in each subject, and paired *t*-tests were used for each SSR to test for significant hemispheric effects on the peak location in each axis.

Scene selectivity

Besides peak activation, we evaluated interhemispheric differences in scene selectivity for each SSR with an adaptive procedure, to avoid error related to using a fixed threshold, and to ensure equivalent signal-to-noise ratios across hemispheres. First, we set the statistical threshold adaptively for individuals so that it corresponded to a fixed number of voxels in each subject and each ROI. Specifically, ROIs were defined with a region growing algorithm which used the local maximum (i.e., peak activation) within a manually delineated SSR as a seed, and then grew regions around the peak by incorporating neighboring voxels, one voxel at a time, in decreasing order of voxel intensity, until reaching the specified region size. Second, instead of one region size, we ran our analysis on a wide range of ROI sizes, including 1, 20, 40, 60, 80, 100, 150, 200, 250, and 300 voxels. Third, scene selectivity for each generated SSR was calculated as the averaged PSC values across voxels within the region. Finally, a standard laterality index (LI) was used to quantify the interhemispheric differences in scene selectivity:

$$\mathrm{LI}=\frac{S_\mathrm{R}-S_\mathrm{L}}{S_\mathrm{R}+S_\mathrm{L}}$$

where S_L and S_R refer to the scene selectivity for homotopic regions from the left (L) and right (R) hemisphere, respectively. A positive value of LI indicated rightward asymmetry (i.e., R > L) and a negative value leftward asymmetry (i.e., L > R). The statistical significance of LI was assessed with one-sample *t*-tests after the step-distributed LI values were normalized using the Fisher transform. Multiple comparisons were corrected with FDR ($q < 0.05$). Note that, in calculating the LI of each SSR, only subjects who had that SSR in both hemispheres were included.

Sex Differences in SSRs

As with interhemispheric differences, sex differences within the SSRs were assessed based on the location of peak activation and scene selectivity. Specifically, sex differences in each SSR were quantified with Cohen's *d* for the peak location or scene selectivity. Cohen's *d* was defined as the difference between sex-specific means of the quantity of interest divided by the pooled standard deviation of the sample population:

$$d=\frac{\bar{X}_\mathrm{f}-\bar{X}_\mathrm{m}}{s}$$

where $s=\sqrt{\frac{(n_\mathrm{f}-1)s_\mathrm{f}^2+(n_\mathrm{m}-1)s_\mathrm{m}^2}{n_\mathrm{f}+n_\mathrm{m}}}$, $\bar{X}$ and s are the mean and standard deviation of the quantity of interest for an SSR, and n refers to the number of females (f) and males (m). An independent two-sample *t*-test was used to test the statistical significance of sex differences.

In addition, the sex differences in the interindividual variability in peak location and the interhemispheric variability in both peak location and scene selectivity were tested for each SSR. Specifically, permutation tests were used to test the significance of sex effects on the interindividual variability of the peak locations. And two-sample *t*-tests were used to test the sex effects on the interhemispheric variability in peak locations and scene selectivity.

RESULTS

As shown in Figure 1A, across individual brains, scene-selective activation varied dramatically in location, extent, and magnitude. Overall, the SSRs were successfully delineated in a large proportion of subjects: PPA (RH: 97.5%, and LH: 97.5%), RSC (RH: 96.5%, and LH: 98.0%), and TOS (RH: 89.1%, and LH: 89.6%) (Table I). The corresponding PPA and RSC delineated from the representative individual activation map provided in Figure 1A are presented in Figure 1B (for the TOS, see Supporting Information Fig. S2), and exemplify interindividual variability of the SSRs in both location and extent.

Reliability for the Delineation of SSRs

As measured using the Dice coefficient (Fig. 2), the manual delineations showed both high intra-rater reliability and high inter-rater reliability. No significant difference between inter- and intra-rater reliabilities was found ($P > 0.05$, Bonferroni correction). Dice coefficients exceeded 0.8 for all three SSRs, and the PPA in particular showed the highest reliability, with both Dice coefficients greater than 0.9. These results indicate excellent intra- and inter-rater agreement in the manual delineations.

Interindividual Variability of SSRs

To quantify interindividual variability in the spatial topography of each SSR, we created a probabilistic atlas

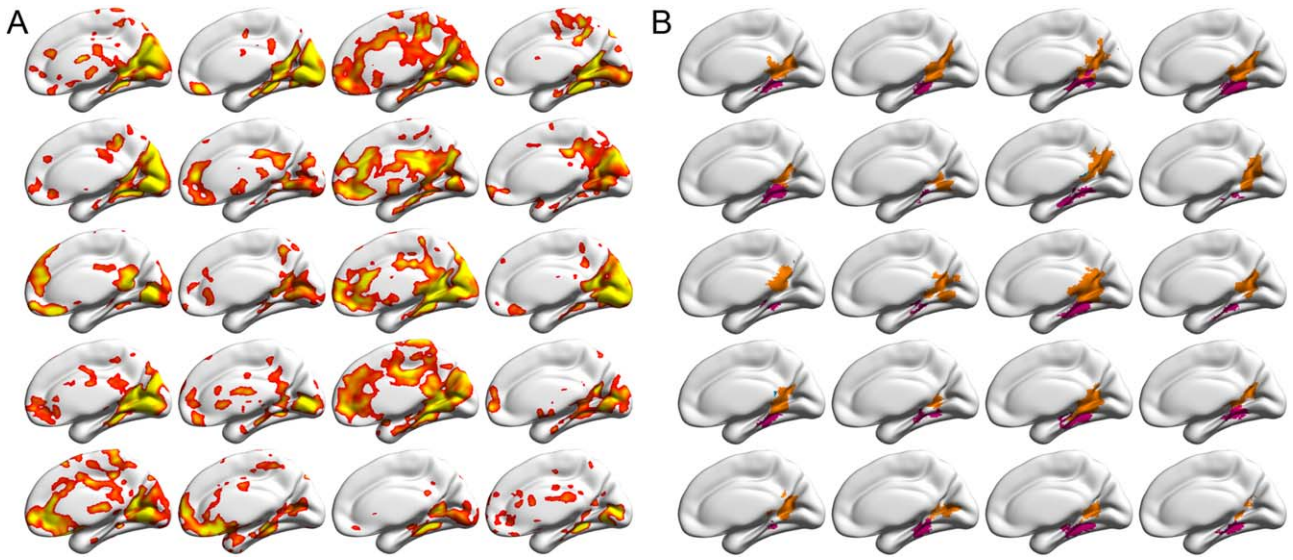

Figure 1.

Sample activations and delineated SSRs in the right hemispheres from the 20 randomly selected brains, overlaid on the standard MNI152 cortical surfaces. Because of space limitations, only the medial view is presented. For the lateral view, see Supporting Information Figure S2. (A) The individual activation maps for the contrast between scenes and objects, derived from three runs of fMRI data for each subject, uncorrected $P < 0.01$ (right-tailed). (B) The delineated subject-specific SSRs for the activations in (A). PPA and RSC were shown in magenta and orange, respectively. Each cell corresponds to one subject. Abbreviations: PPA, parahippocampal place area; RSC, retrosplenial cortex; SSR, scene-selective region. [Color figure can be viewed at wileyonlinelibrary.com]

for each one. As shown in Figure 3A, no voxel (i.e., 100% certainty) was constantly identified as belonging to one specific SSR. The maximum probability of a particular voxel belonging to an SSR ranged from 0.39 to 0.90 (Table I). As expected, high probability was always found in the center of the SSR. In addition, the central voxels showed higher probability in the right hemisphere than those in the left hemisphere for the RSC and TOS, whereas the reverse was observed for the PPA (Fig. 3A), suggesting that spatial variability is different across regions and hemispheres. Because the probabilistic maps of adjacent SSRs (e.g., PPA and RSC) overlapped to some degree in the periphery, a maximum-probability map (MPM) was then created to obtain an integrated, non-overlapping map for all SSRs. As shown in Figure 3B, the MPM revealed a clear topographical relationship between these SSRs. On the medial surface, the PPA was located on the lips of the collateral sulcus and the parahippocampal gyrus, and abutted the medial fusiform gyrus. The RSC occupied the retrosplenial cortex, reaching to the PPA ventrally, and extending superiorly along the parieto-occipital sulcus. On the dorsal surface, the TOS occupied the lateral occipital gyrus and the transverse occipital sulcus.

Interindividual spatial variability was further characterized through measuring the dispersion of the stereotaxic coordinates of a given SSRs peak activation.

TABLE I. Characterization of scene-selective regions: maximum probability, coordinates, and selectivity

Region name	Percent subjects	Maximum probability	MNI peak coordinates mean (SD)			Peak selectivity mean (SD)
			X	Y	Z	
R PPA	97.52	0.83	26 (5)	−43 (5)	−11 (4)	0.93 (0.41)
L PPA	97.52	0.90	−25 (4)	−46 (5)	−10 (4)	0.94 (0.36)
R RSC	96.53	0.77	15 (6)	−54 (6)	8 (8)	1.04 (0.47)
L RSC	98.02	0.72	−13 (6)	−58 (7)	8 (8)	1.16 (0.60)
R TOS	89.11	0.41	48(6)	−70 (9)	32 (8)	0.92 (0.37)
L TOS	89.60	0.39	−42(7)	−76 (9)	33 (8)	0.83 (0.37)

Abbreviations: PPA, parahippocampal place area; RSC, retrosplenial cortex; TOS, transverse occipital sulcus; L, left; R, right.

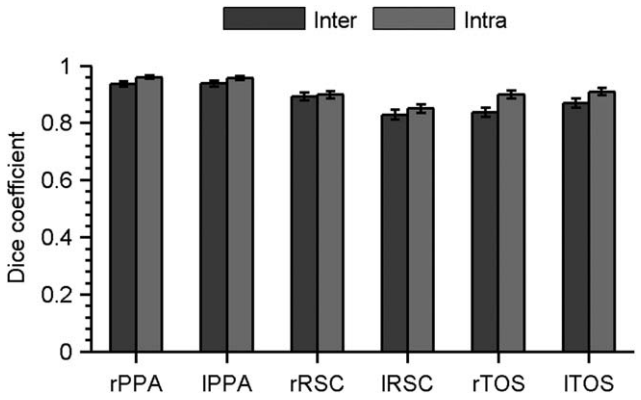

Figure 2.

Intra-rater and inter-rater reliability for the delineation of SSRs measured by the Dice coefficient. A value of 1.0 indicates identical sets of voxels in two labels, while 0.0 represents completely different sets of voxels. The reliability was calculated separately for the right and left SSRs. Abbreviations: PPA, parahippocampal place area; RSC, retrosplenial cortex; SSR, scene-selective region; TOS, transverse occipital sulcus; L, left hemisphere; R, right hemisphere.

As expected, substantial interindividual variations in peak location along all three axes were observed. The SDs of peak activation ranged from several millimeters to 1 cm in each axis, for each SSR (Fig. 4A). The sum of the SDs from the three axes was calculated for each SSR to quantify its overall variability. As shown in Figure 4B, the TOS varied the most overall (LH: 22.4 mm, and RH: 23.6 mm), then the RSC (LH: 19.5 mm, and RH: 21.3 mm) and finally the PPA (LH: 13.8 mm, and RH: 12.6 mm). Thus, the peak activation of the SSRs showed significant interindividual variability in spatial topography. The pattern held true for both male and female groups (Supporting Information Fig. S3). No sex differences were observed in the interindividual variability of the peak locations of the SSRs (permutation test, uncorrected Ps > 0.05).

Besides spatial topography, interindividual functional variability was characterized for each SSR according to the magnitude of scene-selective peak activation. As shown in Figure 5, large interquartile ranges (IQR) were observed in scene selectivity for all SSRs, indicating that each SSR had significant interindividual variability in its response (Fig. 5A). When quantified by the CV, across hemispheres the SSRs on average showed CVs around 0.45 (Fig. 5B). Among them, the RSC (RH: 0.45, and LH: 0.52) showed greater variability than the PPA (RH: 0.44, and LH: 0.38) and TOS (RH: 0.40, and LH: 0.44).

Interhemispheric Variability of SSRs

The interhemispheric variability of the SSRs was first characterized based on the peak locations. As shown in Figure 4C, all three SSRs (PPA: t (192) = 2.75, $P = 0.007$, RSC: t (191) = 5.23, $P < 0.001$, and TOS: t (166) = 7.33, $P < 0.001$) showed significantly higher absolute X-coordinates in the right hemisphere than in the left, indicating that they were more laterally localized in the right hemisphere than in the left hemisphere. Similarly, the right PPA (t (192) = 6.75, $P < 0.001$), RSC (t (191) = 6.70, $P < 0.001$), and TOS (t (166) = 5.87, $P < 0.001$) all had higher coordinates in the Y-axis than their left homotopies. Thus, all three SSRs in the right hemisphere were located more laterally and anteriorly than their left hemisphere counterparts. However, in the Z-coordinate, the right PPA (t (192) = −4.93, $P < 0.001$) and TOS (t (166) = −2.39, $P = 0.018$) had lower coordinates in the Z-axis than their left hemisphere homotopies, indicating that those two SRRs were located more inferiorly in the right hemisphere. The RSC showed no significant hemispheric differences in its Z-coordinate (t (191) = 0.33, $P = 0.337$). Male and female groups showed similar patterns of the interhemispheric variability in the peak locations (Supporting Information Fig. S4). That is, no sex by hemisphere interaction was found for the peak location of the SSRs (two-sample t-tests, uncorrected Ps > 0.05)

The interhemispheric variability of each SSR was also evaluated on the basis of scene selectivity with an adaptive procedure (see Materials and Methods). Several interesting outcomes were observed (Fig. 6). First, the SSRs showed significant interhemispheric asymmetry, but in different directions (Fig. 6A). That is, the PPA and RSC showed stronger scene selectivity in the left hemisphere (PPA: $t_{[\min,\ \max]}$ (192) = [−3.93, −0.76], FDR corrected $q < 0.01$; RSC: $t_{[\min,\ \max]}$ (191) = [−3.81, −2.12], FDR corrected $q < 0.01$), while the TOS showed stronger scene selectivity in the right hemisphere ($t_{[\min,\ \max]}$ (166) = [1.24, 3.35], FDR corrected $q < 0.01$). Second, the three SSRs showed significant differences in the magnitude of laterality index (LI). Regardless of the direction, the PPA showed the least hemispheric asymmetry (LI [min, max] = [−0.04, −0.008]), the TOS in the middle (LI [min, max] = [0.02, 0.05]), and the RSC showed the highest magnitude of LIs (LI [min, max] = [−0.05, −0.04]). Finally, although the selectivity of the SSRs did dramatically change with ROI size, the sign (direction) of LIs stayed the same and the magnitude of LIs changed little, indicating that the interhemispheric differences in scene selectivity were very stable (Fig. 6B). In addition, no significant difference of the LI were observed between left- and right-handers (FDR corrected $q > 0.05$; see Supporting Information Table S1 for details), suggesting that handedness had little effect on interhemispheric differences.

Sex Difference in SSRs

Sex differences within each SSR were also characterized using peak locations and scene selectivity. No significant sex differences were found in the peak location of any SSR (Ps > 0.05). However, males demonstrated higher scene

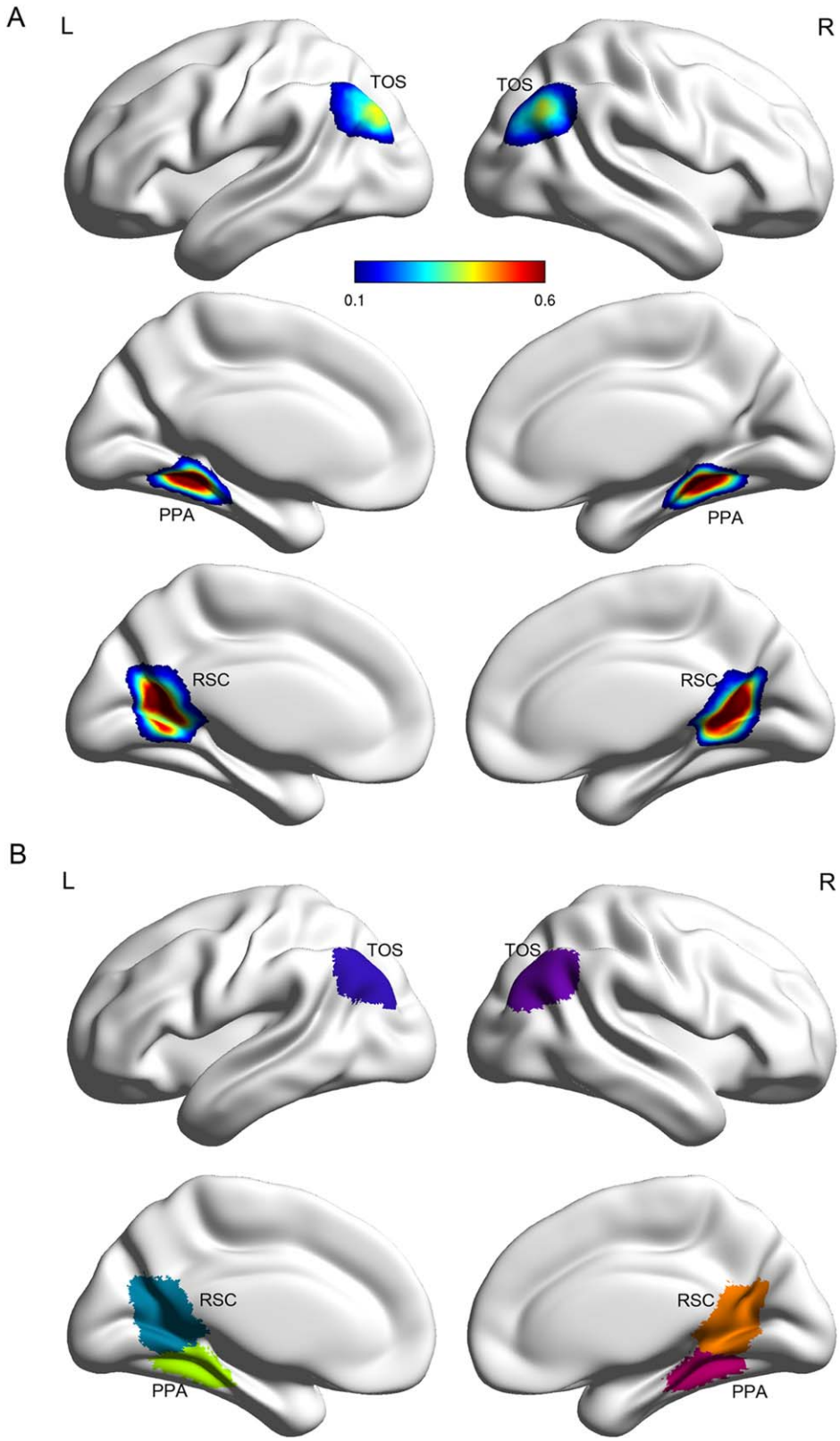

Figure 3.

Probabilistic atlas and maximum probability map for the SSRs. (A) Probabilistic atlas displayed on the standard MNI152 cortical surface. The probability was calculated as the frequency of a respective SSR presented at a given position across all subjects. (B) Maximum probability map visualized as overlays on the MNI152 cortical surface. The value for voxels in which the maximal probability was smaller than 0.1 was set to zero, indicating that they most likely did not belong to any SSRs. Abbreviations: PPA, parahippocampal place area; RSC, retrosplenial cortex; SSR, scene-selective region; TOS, transverse occipital sulcus; L, left hemisphere; R, right hemisphere.

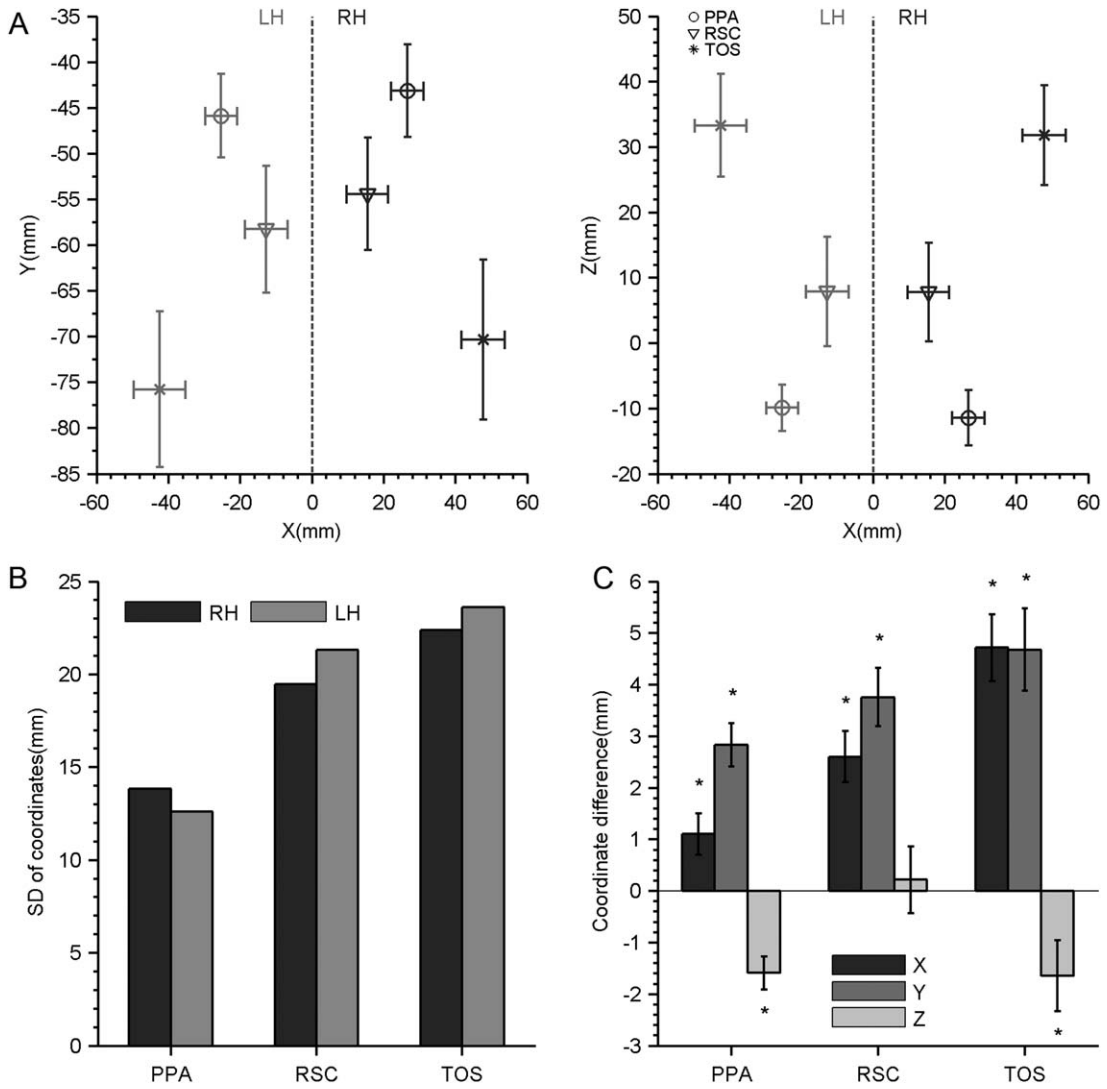

Figure 4.

The interindividual and interhemispheric variability for the location of peak activation. (A) The mean coordinates (mm) and standard deviations (SDs) of the peak activation in the SSRs calculated from the individual brains in the axial (left) and coronal (right) planes. (B) Interindividual variations for the location of peak activation, quantified by the sum of SD from the three coordinate axes. (C) Interhemispheric differences for the location of peak activation, quantified by the coordinate differences on each coordinate axis. Asterisks indicate $P < 0.05$. Abbreviations: PPA, parahippocampal place area; RSC, retrosplenial cortex; SSR, scene-selective region; TOS, transverse occipital sulcus; LH, left hemisphere; RH, right hemisphere.

selectivity than females in all three SSRs (Fig. 7). Specifically, a medium/large sex difference was observed in the PPA (Cohen's $d_{[\min,\ \max]} = [0.43, 0.63]$, $t_{[\min,\ \max]}\ (191) = [3.0, 4.49]$, FDR corrected $q < 0.05$) and TOS (Cohen's $d_{[\min,\ \max]} = [0.53, 0.60]$, $t_{[\min,\ \max]}\ (165) = [3.49, 4.01]$, FDR corrected $q < 0.05$). A small sex difference was observed in the RSC (Cohen's $d_{[\min,\ \max]} = [0.30, 0.35]$), but was no longer significant after the multiple testing corrections ($t_{[\min,\ \max]}\ (190) = [2.0, 3.4]$, FDR corrected $q > 0.05$). Similar to the interhemispheric differences, sex differences in scene selectivity were minimally affected by ROI size, indicating the sex differences identified were very reliable (Fig. 7B). Two-sample t-tests were conducted to test whether there were significant differences in the hemispheric asymmetry between females and males (i.e., an interaction between sex and hemisphere), and no significant interactions were identified in any SSR (FDR corrected $q > 0.05$; see Supporting Information Table S2 for details).

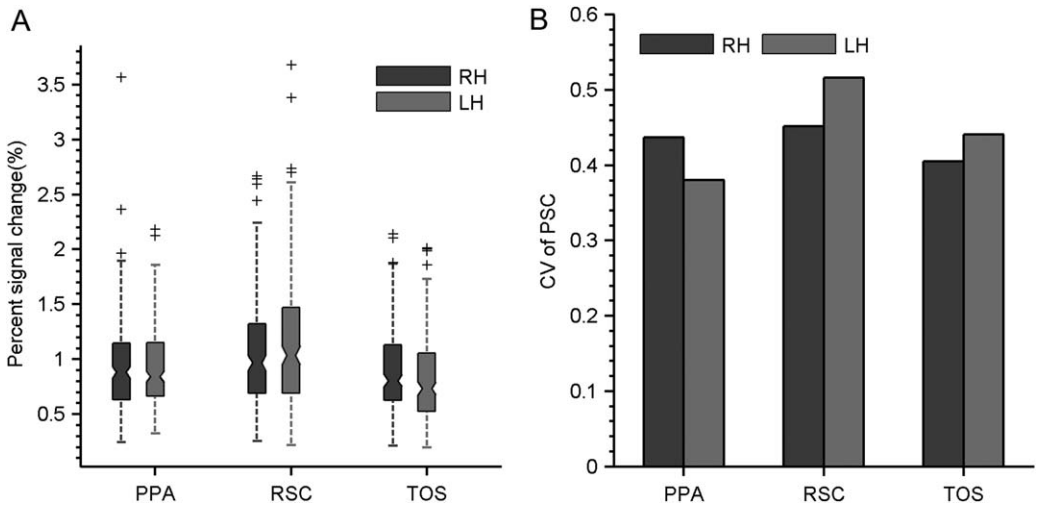

Figure 5.

The interindividual variability of scene selectivity. (A) The distribution of scene selectivity was summarized by a boxplot for each SSR. (B) Interindividual variation in scene selectivity quantified by the coefficient of variation. Abbreviations: PPA, parahippocampal place area; RSC, retrosplenial cortex; SSR, scene-selective region; TOS, transverse occipital sulcus; LH, left hemisphere; RH, right hemisphere.

DISCUSSION

Here, by delineating the subject-specific SSRs in a large sample of subjects, we revealed three aspects of their variability. First, the SSRs showed considerable interindividual variability in both spatial topography and functional selectivity. Second, they showed significant interhemispheric differences in spatial topography and functional selectivity. Finally, the SSRs exhibited significant sex differences in functional selectivity. In addition, the probabilistic atlas was created to quantify the variability of SSRs, which contained precise stereotaxic information on interindividual and interhemispheric differences.

Interindividual Variability of SSRs

Although it is widely acknowledged that there exists a considerable degree of interindividual spatial variability in the functionally-defined regions, to the best of our knowledge, only one study has noted interindividual spatial variability in SSRs, where Frost and Goebel [2012] revealed that the PPA demonstrated significant spatial variability through constructing the probabilistic atlases of the PPA based on a small sample size ($N = 10$). With a large cohort of subjects, we extended this previous study in two ways. First, our probability atlas included the RSC and TOS, not just the PPA. The atlases provide a comprehensive anatomical reference for the SSRs, and thus serve as a useful repository of knowledge and facilitate the mapping of scene-related brain networks. For example, the maps could be used as norms to distinguish normal and pathological variations, or to serve as spatial priors in identifying SSRs in new subjects. Second, we quantified the spatial variability in more detail, and identified more than 20 mm divergence in the location of peak activation across subjects, almost twice that in the face-selective regions (FSR) [Zhen et al., 2015]. Taken together, we provided the first comprehensive characterization of the interindividual spatial variability for the three most-studied SSRs.

Besides spatial topography, the SSRs showed significant interindividual variability in functional selectivity. Previous studies have revealed remarkable variability in scene selectivity, though most of these studies have not been studied in detail [Bettencourt and Xu, 2013; Julian et al., 2012; Kornblith et al., 2013; Nasr et al., 2011]. We observed that the SSRs we studied showed remarkable variability in their scene selectivity (CV = ~0.45), which again is nearly twice that seen for faces in FSRs (CV = ~0.25) [Zhen et al., 2015]. Interestingly, we noticed that the SSRs showed larger interindividual variability than the FSRs in both spatial topography and functional selectivity. Why the distribution of this variability is regionally non-uniform remains unclear, but one possibility is that natural scenes are themselves more variable than well-structured faces. Further studies are needed to elucidate the reason for the described regional differences identified herein.

The behavioral relevance of interindividual variability in the SSRs has yet to be widely studied. However, some studies on other functional regions (e.g., FSRs) have demonstrated that interindividual spatial and selectivity variability of functional regions likely provides a neural basis

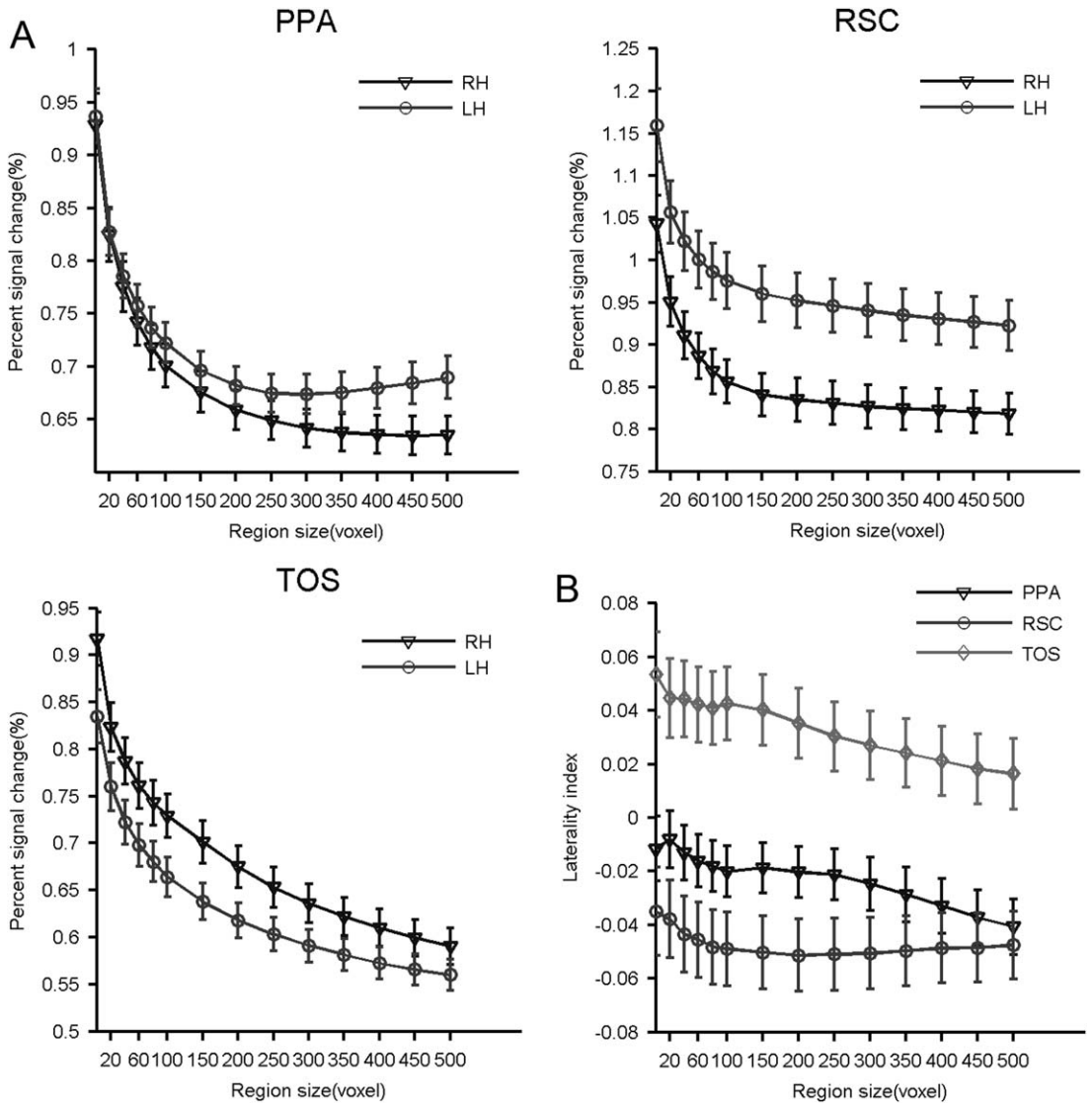

Figure 6.

Interhemispheric differences in the scene selectivity of each SSR, measured at different region sizes. (A) The scene selectivity of SSRs from the right and left hemispheres. (B) The effect size of the interhemispheric differences calculated by the laterality index. Abbreviations: PPA, parahippocampal place area; RSC, retrosplenial cortex; SSR, scene-selective region; TOS, transverse occipital sulcus; LH, left hemisphere; RH, right hemisphere.

for interindividual differences in behavioral performance. For example, Scherf et al. [2010] finds that the spatial topography of face-related cortex is selectively disrupted in autism. Furl et al. [2011] and Huang et al. [2014] demonstrate that individual differences in face selectivity of the OFA and FFA predict differences in face recognition performance. Therefore, the spatial and selectivity variability of the SSRs may likely underlie individual differenced in navigation, especially when scene perception is being utilized. Future studies will be needed to elaborate on the mechanism and functional significance of the interindividual variability of the SSRs and to utilize the variability in understanding the neural mechanisms of scene perception [Kanai and Rees, 2011; Van Horn et al., 2008].

Interhemispheric Differences of SSRs

In addition to interindividual variability, the SSRs presented remarkable interhemispheric variability in both spatial location and functional selectivity. In spatial topography, the three SSRs showed the same pattern in

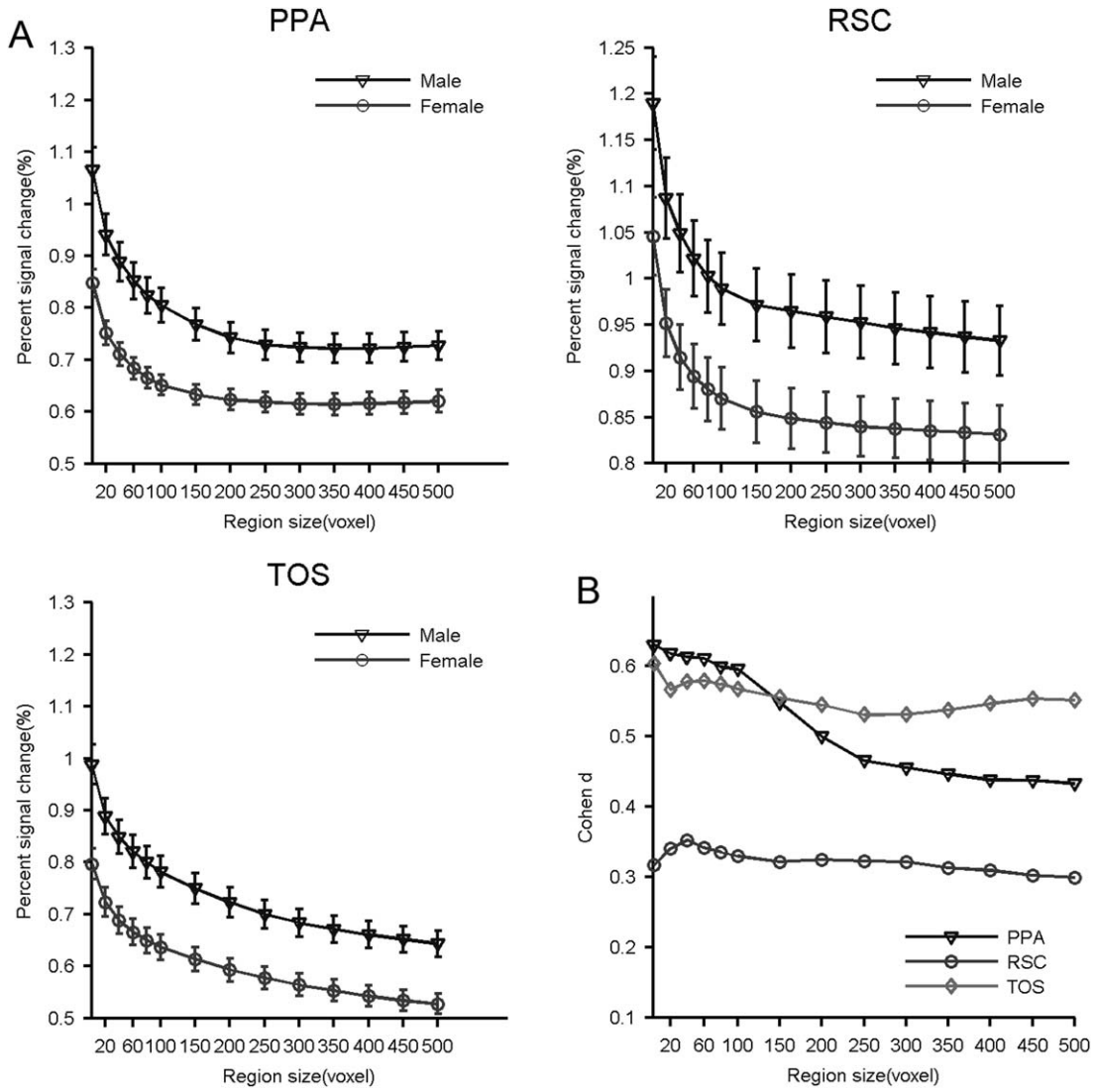

Figure 7.

Sex difference in the scene selectivity of the SSRs measured at different region sizes. (A) Scene selectivity of the SSRs in males and females. (B) The effect size of the sex difference calculated by Cohen's d. Abbreviations: PPA, parahippocampal place area; RSC, retrosplenial cortex; SSR, scene-selective region; TOS, transverse occipital sulcus.

interhemispheric differences: The SSRs in the right hemisphere were more lateral, anterior, and inferior than those in the left hemisphere. The consistent interhemispheric differences in the spatial topography of the three SSRs suggest a different structure-function relationship in the whole scene processing network for each hemisphere. In contrast, the hemispheric asymmetry in scene selectivity is divergent across the SSRs: The PPA and RSC showed a leftward asymmetry, while the TOS showed a rightward asymmetry. Although the magnitude of the interhemispheric difference was small, the present study was designed to ensure the reliability of this finding. First, the interhemispheric difference was measured on a sequence of subject-specific ROIs with different sizes, rather than on a single arbitrary threshold. Therefore, in the calculation of hemispheric differences, the dependence on the choice of threshold was effectively reduced. Second, a large scale fMRI dataset from the same scanner and the same protocol was used to estimate the hemispheric difference, ensuring a large enough sample size to identify subtle differences. It should be noted that the effect size of laterality is small relative to the language areas [Adcock et al., 2003; Desmond et al., 1995] or FSRs [Rossion et al., 2003; Zhen et al., 2015]. So, we cannot simply draw the conclusion that the SSRs are hemisphere-dominant without independent electrophysiological validation of these data.

The functional significance of interhemispheric differences in the SSRs is still largely unknown. One possible reason for the interhemispheric differences may relate to the hemisphere that predominates in processing different spatial frequency information. A number of behavioral and neuroimaging studies suggest that the right hemisphere specializes in processing low spatial frequency (LSF), or global, information, whereas the left hemisphere specializes in processing high spatial frequency (HSF), or local, information [Kauffmann et al., 2014]. Thus, it is plausible that the PPA and RSC mostly process HSF information, while the TOS is focused on LSF information in the scenes. In line with the interpretation, Rajimehr et al. [2011] observes that in humans and macaques, the PPA responds more strongly to HSF than LSF stimuli. Zeidman et al. [2012] also finds that the PPA shows stronger activation in HSF versus LSF spaces when participants have to detect the disappearance of a small proportion of dots. According to the integrative hierarchical model of visual perception [Bar et al., 2006; Bullier, 2001; Kveraga et al., 2007; Peyrin et al., 2010], we can further assume that LSF information may reach TOS first, enabling coarse initial parsing of the visual scene, which can then be sent back through feedback connections into, the PPA and RSC to guide a finer analysis based on HSF. Future studies are needed to test this hypothesis and explore the spatial frequency specialization of SSRs across hemispheres.

Sex Differences of SSRs

We also observed considerable sex differences in the functional selectivity of the SSRs. Males showed greater scene selectivity than females in the three SSRs, though the difference was not significant in the RSC. Although male advantages in spatial navigation have been well documented [Astur et al., 1998; Linn and Petersen, 1985; Lovden et al., 2007; Moffat et al., 1998; Rahman et al., 2005], to our knowledge, few studies have characterized the sex differences of brain activity relevant to these tasks. Worse, these studies produce mixed results in the anatomical landmarks where the SSRs anchor. Gron et al. [2000] reveals that in maze navigation, males show greater activation than females in the right parahippocampal gyrus and left posterior cingulate/retrosplenial cortex. On the other hand, Sneider et al. [2011] finds that women have larger activation during learning the maze navigation in the right parahippocampal gyrus and the cingulate cortex. Finally, Nowak et al. [2011] reports that men show greater activation in the posterior cingulate retrosplenial cortex, but women showed greater activation in the parahippocampal gyrus. Here, based on a large cohort of healthy participants and subject-specific ROI analysis, our study provided the first evidence that significant sex differences exist in the functional selectivity of three well-defined SSRs that are involved in spatial navigation.

Behavioral studies have demonstrated that the two sexes employ different strategies in navigating: Men prefer allocentric (e.g., orientation) strategies and are more adept at using them than women, and women prefer egocentric (e.g., landmark) strategies [e.g., Coluccia and Louse, 2004; Galea and Kimura, 1993; Malinowski and Gillespie, 2001; Rahman et al., 2005]. As the SSRs are mainly responsible for perceiving the local visual environment, we speculate that the sex difference in functional selectivity may partly underlie the male facility in decoding the scenes. In addition, the difference suggests each sex uses a unique mechanism for processing scene information that meets the demands of its preferred visuospatial navigation strategy. Future studies experimentally manipulating strategy and matching men and women on behavioral outcomes within each strategy could better define the effects of sex and strategy on the functional correlates of the SSRs.

Limitations and Future Directions

The present work involves several limitations needed to be addressed in future research. First, the volume-based approach was used to define the individual SSR and generate the probabilistic atlases. The volume-based registration contains no model of the cortical surface, and may fail to match the fine anatomy between subjects. As a result, the residual macro-anatomical variability from volume-based registration may confound the measured spatial variability of the SSRs. Future work with advanced surface-based approach is likely to remove macro-anatomical variability more thoroughly and make the measure for the spatial variability of the functional regions more accurate [Frost and Goebel, 2012, 2013]. Second, the variability was observed from a cohort of homogeneous young adults with a narrow age range, which limits the generalization of the variability observed here to people with different ages, especially children and the elderly. Future studies are needed to characterize how the different aspects of variability in SSRs change with ages. Finally, the interindividual variability of functional regions may root in multiple sources, such as variability in the cytoarchitecture [Zilles and Amunts, 2013], hemodynamic response functions [Aguirre et al. 1998; Handwerker et al. 2004], connectivity patterns [Mueller et al., 2013], functional plasticity [Polley et al., 2006; Song et al., 2010], and genetic factors [Blokland et al., 2011; Koten et al., 2009]. It is notable that the spatial variability of the SSRs seen here is nearly twice that seen for the face-selective regions [Zhen et al., 2015]. How the multiple sources may determine different interindividual variability of the functional regions is another direction worthy of exploration in the future.

CONCLUSION

We observed that the SSRs showed considerable interindividual variability, and interhemispheric and sex differences.

The study advanced our mapping of the variability of the SSRs, and invited future studies to explore the mechanisms underlying the variability and its behavioral significance. Moreover, the full description of these variabilities would help us to frame new hypotheses, and provide new insights into the brain networks utilized for scene recognition and navigation. Finally, the probabilistic atlas of SSRs from this work is freely available (http://www.brainactivityatlas.org), and could serve as a resource for the brain mapping community to further characterize the brain networks involved in scene recognition.

REFERENCES

Adcock JE, Wise RG, Oxbury JM, Oxbury SM, Matthews PM (2003): Quantitative fMRI assessment of the differences in lateralization of language-related brain activation in patients with temporal lobe epilepsy. Neuroimage 18:423–438.

Aguirre GK, Detre JA, Alsop DC, D'Esposito M (1996): The parahippocampus subserves topographical learning in man. Cereb Cortex 6:823–829.

Aguirre GK, Zarahn E, D'Esposito M (1998): The variability of human, BOLD hemodynamic responses. Neuroimage 8: 360–369.

Aminoff EM, Tarr MJ (2015): Associative processing is inherent in scene perception. PLoS One 10:e0128840.

Amunts K, Schleicher A, Burgel U, Mohlberg H, Uylings HB, Zilles K (1999): Broca's region revisited: Cytoarchitecture and intersubject variability. J Comp Neurol 412:319–341.

Astur RS, Ortiz ML, Sutherland RJ (1998): A characterization of performance by men and women in a virtual Morris water task: A large and reliable sex difference. Behav Brain Res 93: 185–190.

Bar M, Aminoff E (2003): Cortical analysis of visual context. Neuron 38:347–358.

Bar M, Kassam KS, Ghuman AS, Boshyan J, Schmid AM, Dale AM, Hamalainen MS, Marinkovic K, Schacter DL, Rosen BR, Halgren E (2006): Top-down facilitation of visual recognition. Proc Natl Acad Sci U S A 103:449–454.

Bettencourt KC, Xu Y (2013): The role of transverse occipital sulcus in scene perception and its relationship to object individuation in inferior intraparietal sulcus. J Cogn Neurosci 25:1711–1722.

Blokland GA, McMahon KL, Thompson PM, Martin NG, de Zubicaray GI, Wright MJ (2011): Heritability of working memory brain activation. J Neurosci 31:10882–10890.

Bullier J (2001): Integrated model of visual processing. Brain Res Brain Res Rev 36:96–107.

Caspers J, Zilles K, Eickhoff SB, Schleicher A, Mohlberg H, Amunts K (2013): Cytoarchitectonical analysis and probabilistic mapping of two extrastriate areas of the human posterior fusiform gyrus. Brain Struct Funct 218:511–526.

Chai XJ, Jacobs LF (2009): Sex differences in directional cue use in a virtual landscape. Behav Neurosci 123:276–283.

Chance SA (2014): The cortical microstructural basis of lateralized cognition: A review. Front Psychol 5:820.

Cherney ID, Brabec CM, Runco DV (2008): Mapping out spatial ability: Sex differences in way-finding navigation. Percept Mot Skills 107:747–760.

Coluccia E, Louse G (2004): Gender differences in spatial orientation: A review. J Environ Psychol 24:329–340.

Desmond JE, Sum JM, Wagner AD, Demb JB, Shear PK, Glover GH, Gabrieli JD, Morrell MJ (1995): Functional MRI measurement of language lateralization in Wada-tested patients. Brain 118 (Pt 6):1411–1419.

Dilks DD, Julian JB, Paunov AM, Kanwisher N (2013): The occipital place area is causally and selectively involved in scene perception. J Neurosci 33:1331–1336.

Epstein R, Harris A, Stanley D, Kanwisher N (1999): The parahippocampal place area: Recognition, navigation, or encoding?. Neuron 23:115–125.

Epstein R, Kanwisher N (1998): A cortical representation of the local visual environment. Nature 392:598–601.

Epstein RA (2008): Parahippocampal and retrosplenial contributions to human spatial navigation. Trends Cogn Sci 12:388–396.

Epstein RA, Parker WE, Feiler AM (2007): Where am I now? Distinct roles for parahippocampal and retrosplenial cortices in place recognition. J Neurosci 27:6141–6149.

Fischl B, Rajendran N, Busa E, Augustinack J, Hinds O, Yeo BT, Mohlberg H, Amunts K, Zilles K (2008): Cortical folding patterns and predicting cytoarchitecture. Cereb Cortex 18:1973–1980.

Fox CJ, Iaria G, Barton JJ (2009): Defining the face processing network: Optimization of the functional localizer in fMRI. Hum Brain Mapp 30:1637–1651.

Frost MA, Goebel R (2012): Measuring structural-functional correspondence: Spatial variability of specialised brain regions after macro-anatomical alignment. Neuroimage 59: 1369–1381.

Frost MA, Goebel R (2013): Functionally informed cortex based alignment: An integrated approach for whole-cortex macro-anatomical and ROI-based functional alignment. Neuroimage 83:1002–1010.

Furl N, Garrido L, Dolan RJ, Driver J, Duchaine B (2011): Fusiform gyrus face selectivity relates to individual differences in facial recognition ability. J Cogn Neurosci 23:1723–1740.

Galea LAM, Kimura D (1993): Sex differences in route-learning. Pers Indiv Differ 14:53–65.

Gotts SJ, Jo HJ, Wallace GL, Saad ZS, Cox RW, Martin A (2013): Two distinct forms of functional lateralization in the human brain. Proc Natl Acad Sci U S A 110:E3435–E3444.

Grill-Spector K (2003): The neural basis of object perception. Curr Opin Neurobiol 13:159–166.

Gron G, Wunderlich AP, Spitzer M, Tomczak R, Riepe MW (2000): Brain activation during human navigation: Gender-different neural networks as substrate of performance. Nat Neurosci 3:404–408.

Handwerker DA, Ollinger JM, D'Esposito M (2004): Variation of BOLD hemodynamic responses across subjects and brain regions and their effects on statistical analyses. Neuroimage 21:1639–1651.

Hellige JB (1990): Hemispheric asymmetry. Annu Rev Psychol 41: 55–80.

Henderson JM, Larson CL, Zhu DC (2008): Full scenes produce more activation than close-up scenes and scene-diagnostic objects in parahippocampal and retrosplenial cortex: An fMRI study. Brain Cogn 66:40–49.

Herve PY, Zago L, Petit L, Mazoyer B, Tzourio-Mazoyer N (2013): Revisiting human hemispheric specialization with neuroimaging. Trends Cogn Sci 17:69–80.

Hill J, Dierker D, Neil J, Inder T, Knutsen A, Harwell J, Coalson T, Van Essen D (2010): A surface-based analysis of hemispheric asymmetries and folding of cerebral cortex in term-born human infants. J Neurosci 30:2268–2276.

Huang L, Song Y, Li J, Zhen Z, Yang Z, Liu J (2014): Individual differences in cortical face selectivity predict behavioral performance in face recognition. Front Hum Neurosci 8:483.

Hugdahl K (2011): Hemispheric asymmetry: Contributions from brain imaging. Wiley Interdiscip Rev Cogn Sci 2:461–478.

Jager G, Postma A (2003): On the hemispheric specialization for categorical and coordinate spatial relations: A review of the current evidence. Neuropsychologia 41:504–515.

Julian JB, Fedorenko E, Webster J, Kanwisher N (2012): An algorithmic method for functionally defining regions of interest in the ventral visual pathway. Neuroimage 60:2357–2364.

Kanai R, Rees G (2011): The structural basis of inter-individual differences in human behaviour and cognition. Nat Rev Neurosci 12:231–242.

Kauffmann L, Ramanoel S, Peyrin C (2014): The neural bases of spatial frequency processing during scene perception. Front Integr Neurosci 8:37.

Kornblith S, Cheng X, Ohayon S, Tsao DY (2013): A network for scene processing in the macaque temporal lobe. Neuron 79: 766–781.

Koten JW, Jr, Wood G, Hagoort P, Goebel R, Propping P, Willmes K, Boomsma DI (2009): Genetic contribution to variation in cognitive function: An FMRI study in twins. Science 323:1737–1740.

Kravitz DJ, Peng CS, Baker CI (2011): Real-world scene representations in high-level visual cortex: It's the spaces more than the places. J Neurosci 31:7322–7333.

Kveraga K, Ghuman AS, Bar M (2007): Top-down predictions in the cognitive brain. Brain Cogn 65:145–168.

Linn MC, Petersen AC (1985): Emergence and characterization of sex differences in spatial ability: A meta-analysis. Child Dev 56:1479–1498.

Lovden M, Herlitz A, Schellenbach M, Grossman-Hutter B, Kruger A, Lindenberger U (2007): Quantitative and qualitative sex differences in spatial navigation. Scand J Psychol 48:353–358.

MacEvoy SP, Epstein RA (2007): Position selectivity in scene- and object-responsive occipitotemporal regions. J Neurophysiol 98: 2089–2098.

Maguire EA (2001): The retrosplenial contribution to human navigation: A review of lesion and neuroimaging findings. Scand J Psychol 42:225–238.

Maguire EA, Frackowiak RS, Frith CD (1997): Recalling routes around london: Activation of the right hippocampus in taxi drivers. J Neurosci 17:7103–7110.

Maguire EA, Gadian DG, Johnsrude IS, Good CD, Ashburner J, Frackowiak RS, Frith CD (2000): Navigation-related structural change in the hippocampi of taxi drivers. Proc Natl Acad Sci U S A 97:4398–4403.

Maguire EA, Woollett K, Spiers HJ (2006): London taxi drivers and bus drivers: A structural MRI and neuropsychological analysis. Hippocampus 16:1091–1101.

Malinowski JC, Gillespie WT (2001): Individual differences in performance on a large-scale, real-world wayfinding task. J Environ Psychol 21:73–82.

Meyer F (1994): Topographic distance and watershed lines. Signal Process 38:113–125.

Moffat SD, Hampson E, Hatzipantelis M (1998): Navigation in a "virtual" maze: Sex differences and correlation with psychometric measures of spatial ability in humans. Evol Hum Behav 19:73–87.

Mueller S, Wang D, Fox MD, Yeo BT, Sepulcre J, Sabuncu MR, Shafee R, Lu J, Liu H (2013): Individual variability in functional connectivity architecture of the human brain. Neuron 77:586–595.

Nasr S, Liu N, Devaney KJ, Yue X, Rajimehr R, Ungerleider LG, Tootell RB (2011): Scene-selective cortical regions in human and nonhuman primates. J Neurosci 31:13771–13785.

Nowak N, Resnick S, Elkins W, Moffat S (2011): Sex differences in brain activation during virtual navigation: A functional MRI study. In: Carlson L, Hoelscher C, Shipley TF, editors. Proceedings of the 33rd Annual Meeting of the Cognitive Science Society: Austin, TX: Cognitive Science Society. pp 2776–2781.

Park S, Brady TF, Greene MR, Oliva A (2011): Disentangling scene content from spatial boundary: Complementary roles for the parahippocampal place area and lateral occipital complex in representing real-world scenes. J Neurosci 31:1333–1340.

Persson J, Spreng RN, Turner G, Herlitz A, Morell A, Stening E, Wahlund LO, Wikstrom J, Soderlund H (2014): Sex differences in volume and structural covariance of the anterior and posterior hippocampus. Neuroimage 99:215–225.

Peyrin C, Michel CM, Schwartz S, Thut G, Seghier M, Landis T, Marendaz C, Vuilleumier P (2010): The neural substrates and timing of top-down processes during coarse-to-fine categorization of visual scenes: A combined fMRI and ERP study. J Cogn Neurosci 22:2768–2780.

Pitcher D, Dilks DD, Saxe RR, Triantafyllou C, Kanwisher N (2011): Differential selectivity for dynamic versus static information in face-selective cortical regions. Neuroimage 56:2356–2363.

Polley DB, Steinberg EE, Merzenich MM (2006): Perceptual learning directs auditory cortical map reorganization through top-down influences. J Neurosci 26:4970–4982.

Rahman Q, Andersson D, Govier E (2005): A specific sexual orientation-related difference in navigation strategy. Behav Neurosci 119:311–316.

Rajimehr R, Devaney KJ, Bilenko NY, Young JC, Tootell RB (2011): The "parahippocampal place area" responds preferentially to high spatial frequencies in humans and monkeys. PLoS Biol 9:e1000608.

Rossion B, Joyce CA, Cottrell GW, Tarr MJ (2003): Early lateralization and orientation tuning for face, word, and object processing in the visual cortex. Neuroimage 20:1609–1624.

Scheperjans F, Eickhoff SB, Homke L, Mohlberg H, Hermann K, Amunts K, Zilles K (2008): Probabilistic maps, morphometry, and variability of cytoarchitectonic areas in the human superior parietal cortex. Cereb Cortex 18:2141–2157.

Scherf KS, Luna B, Minshew N, Behrmann M (2010): Location, location, location: Alterations in the functional topography of face- but not object- or place-related cortex in adolescents with autism. Front Hum Neurosci 4:26.

Schinazi VR, Nardi D, Newcombe NS, Shipley TF, Epstein RA (2013): Hippocampal size predicts rapid learning of a cognitive map in humans. Hippocampus 23:515–528.

Sneider JT, Sava S, Rogowska J, Yurgelun-Todd DA (2011): A preliminary study of sex differences in brain activation during a spatial navigation task in healthy adults. Percept Mot Skills 113:461–480.

Song Y, Hu S, Li X, Li W, Liu J (2010): The role of top-down task context in learning to perceive objects. J Neurosci 30:9869–9876.

Suzuki K, Yamadori A, Hayakawa Y, Fujii T (1998): Pure topographical disorientation related to dysfunction of the viewpoint dependent visual system. Cortex 34:589–599.

Toga AW, Thompson PM (2003): Mapping brain asymmetry. Nat Rev Neurosci 4:37–48.

Van der Ham IJ, van Zandvoort MJ, Frijns CJ, Kappelle LJ, Postma A (2011): Hemispheric differences in spatial relation processing in a scene perception task: A neuropsychological study. Neuropsychologia 49:999–1005.

Van Essen DC, Dierker DL (2007): Surface-based and probabilistic atlases of primate cerebral cortex. Neuron 56: 209–225.

Van Horn JD, Grafton ST, Miller MB (2008): Individual variability in brain activity: A nuisance or an opportunity?. Brain Imaging Behav 2:327–334.

Wolbers T, Buchel C (2005): Dissociable retrosplenial and hippocampal contributions to successful formation of survey representations. J Neurosci 25:3333–3340.

Zeidman P, Mullally SL, Schwarzkopf DS, Maguire EA (2012): Exploring the parahippocampal cortex response to high and low spatial frequency spaces. Neuroreport 23:503–507.

Zhen Z, Yang Z, Huang L, Kong XZ, Wang X, Dang X, Huang Y, Song Y, Liu J (2015): Quantifying interindividual variability and asymmetry of face-selective regions: A probabilistic functional atlas. NeuroImage 113:13–25.

Zilles K, Amunts K (2013): Individual variability is not noise. Trends Cogn Sci 17:153–155.